Punjab University
Journal of Mathematics (ISSN 1016-2526)
Vol.47(2)(2015) pp. 11-18

Simulation of Drug Diffusion in Mammalian Cell

Misbah Gul
Department of Mathematics,
University of Sargodha, Lahore Campus, Pakistan
Email: misbahahmad40@yahoo.com

Qasim Ali Chaudhry, Naima Abid and Saira Zahid
Department of Mathematics,
University of Engineering and Technology, Lahore
Emails: alicq@kth.se, naimakhan25@gmail.com, sairazahid71@gmail.com

Received: 15 February, 2015 / Accepted: 10 April, 2015 / Published online: 17 September, 2015

Abstract. Scores of intricate problems are churned out in mammalian cell owing to the influence of lipophilic aromatic hydrocarbons. Diffusion and reaction of these noxious compounds obliterate the cellular structure. Earlier, a mathematical model was developed which gives rise to a system of PDEs. This system was treated numerically. Homogenization technique was used for the numerical treatment of cytoplasm which reduced the complexity of the model. The disparity in the formation of tetrols guides us towards a new model comprising nuclear envelope, enzymatic reactions and modifying the nuclear size. The results of the model are compared with previous model and experimental results of V79 cells, which show a significant improvement in the model.

AMS (MOS) Subject Classification Codes: 65M08; 92B05; 92C37; 92C45
Key Words: Mammalian cell, Diffusion and reaction, PDEs, Homogenization, V79.

3. Introduction

Cell is the essential structural and functional unit of living organisms. Eyokaryotic cell consists of plasma membrane, cytoplasm, mitochondria, Golgi apparatus, endoplasmic Reticulum, nuclear envelope and nucleus consisting of most important DNA [2]. Modeling the intracellular dynamics is a very difficult task due to

complex membranous structure. PAH [17], a ubiquitous environmental pollutant, diffuses into the cell and reacts with different compounds which may cause toxicity and cancer [1,13]. To study the chemical reactions and diffusion process in a cell, a 2D-axisymmetric mathematical model was earlier developed in [10]. In this model, extracellular medium along with four sub-domains namely cellular membrane, cytoplasm, nuclear membrane and cytoplasm were considered. The reaction and diffusion processes in the whole cell model gave rise to the system of partial differential equations which was treated numerically. Geometry of cytoplasm is very complex. It contains very dense structure of cellular organelles and membranes. Numerically, it is almost impossible to model these organelles independently because the system becomes computationally very expensive. In order to treat the model numerically and keeping in view the limitations of computational sources, homogenization technique was used where the effective equations were derived. In this paper, we will use the results of the effective equations which were derived earlier in [10]. In the present study, a 2D axi-symmetric model is extended by reducing the size of nucleus and introducing nuclear envelope. Nuclear envelope encloses the heart of the cell called nucleus. The nuclear envelope consists of two concentric membranes, i.e. outer and inner membranes. The two layers are separated by 30nm space known as perinuclear space. Outer membrane is composed of protein endoplasmic reticulum. Inner and outer membranes fuse periodically to form nuclear pore complexes. These nuclear pores work as a bridge for the access to different diffusing materials. They also control the movement of molecules between cytoplasm and nucleus. Nuclear envelope is not only a double layered membrane, it is a highly structured organelle that works as an interface between cytoplasm and nucleus region. It also maintains the nucleus shape and is helpful in DNA replication, nuclear growth, protein synthesis and processing [5,18].

4. Material And Methods

The mathematical model describes the diffusion and reaction process of the toxic compound BPDE which was earlier used in [10] named as P in this model.

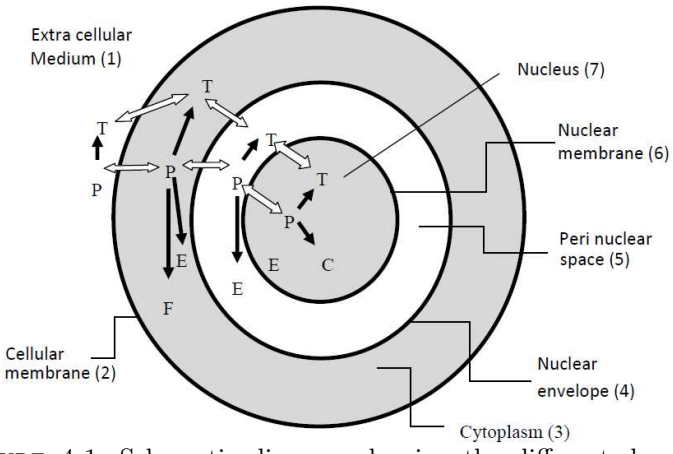

Figure 4.1. Schematic diagram showing the different domains and reaction-diffusion

It is formed by incomplete incineration of hydrocarbons in oil refining and other such activities [16]. The model geometry consists of sub domains; extracellular medium, plasma membrane, cytoplasm, perinuclear space, nuclear membrane and nucleus. No reaction occurs in membranous structure. In extracellular medium, P endures hydrolysis process to form tetrol. Inside cytoplasm three types of reactions take place; one is hydrolysis which yields tetrol, second is the reaction of P with glutathione (GSH) in the presence of glutathione transferases (GSTs) which serve as catalyst forming DE-GSH conjugate [9] and third is the reaction of P with proteins which form protein adducts. P diffuses into the perinuclear space and reacts with protein bindings to form protein adduct [11]. P also reaches in the nucleus; reacts with water, DNA and protein to form tetrols, DNA adduct and protein adduct respectively [14]. Reaction of P with DNA may destroy its structure [20]. Schematic diagram showing the different domains and reaction-diffusion process is shown in Fig. 2.1. Formation of DNA adducts may result in mutation and a cause of tumor or cancer. The main reactant BPDE is extremely lipophilic in nature and the membranes have also lipophilic behavior so its major part is absorbed in membrane. The rapid change in the concentration between adjacent lipid and water domain can be explained by the partition coefficient K_p. The geometric constants used in this model are given in Table-1.

TABLE 1. Fundamental geometric constants

Constants	**Value**
Volume of one cell[m^3]	3×10^{-15}
Thickness of membrane	1.13×10^{-8}
Volume of cell/volume of nucleus	10
Volume of cell medium for 1.5×10^7cells	10^{-5}
Thickness of perinuclear space[m]	30×10^{-9}

The distribution of the material in each domain is defined by concentration. The concentration in each domain is separated by using an index i. for example Pi shows the concentration of P in particular subdomain i, D represents the diffusion coefficient and KT represents the reaction rate constant.

Sub-domain 1(extracellular medium)

$$\frac{\partial}{\partial t}P_1 = \nabla \cdot (D_1 \nabla P_1) - K_T P_1, \tag{4.1}$$

$$\frac{\partial}{\partial t}T_1 = \nabla \cdot (D_1 \nabla T_1) + K_T P_1. \tag{4.2}$$

where P_1 and T_1 represent the BPDE and tetrols respectively in the sub-domain 1. D1 stands for the diffusion process in this sub-domain. The subscript '1' denotes the sub-domain number. K_T represents the rate constant for the formation of tetrols.

The first part of the equations represents the diffusion part whereas the second part shows the reaction phenomenon.

Sub-domains 2, 4, 6 (cellular membrane, nuclear envelope, nuclear membrane)

$$\frac{\partial}{\partial t}P_i = \nabla \cdot (D_i \nabla P_i), \tag{4.3}$$

$$\frac{\partial}{\partial t}T_i = \nabla \cdot (D_i \nabla T_i), \quad i = 2, 4, 6 \tag{4.4}$$

In this sub-domain, we have not considered any reaction in the membranous part of the model, therefore only diffusion factor appeared in the equations.

Sub-domain 3 (cytoplasm)

The structure of cytoplasm is very complex. It consists of water and lipid membranes. If we observe the diffusion and reaction mechanism in each sub domain separately the model will become computationally very expensive. In order to avoid this, effective equations are used which were derived earlier in [10] by using homogenization technique, the details of which are given there. During the process of homogenization, effective diffusion coefficients and chemical rate constants for cytoplasm were calculated in [10] and are summarized in Table 2. The remaining physical and chemical constants were used from [10,15,19,22] and are given in Table 2. The reaction rate constants are given by $K_{T,\text{eff}}$ and $K_{F,\text{eff}}$. The following reactions take place in cytoplasm.

$$P \xrightarrow{K_{T,\text{eff}}} T \qquad , \qquad P \xrightarrow{K_{F,\text{eff}}} F \qquad , \qquad P \xrightarrow{K_{E,\text{eff}}} E$$

The following equations are obtained from the set of above chemical reactions

$$\sigma_P \frac{\partial}{\partial t}P_3 = \nabla \cdot (D_{3,P,\text{eff}} \nabla P_3) - (K_{T,\text{eff}} + K_{F,\text{eff}} + K_{E,\text{eff}})P_3, \tag{4.5}$$

$$\sigma_T \frac{\partial}{\partial t}T_3 = \nabla \cdot (D_{3,T,\text{eff}} \nabla P_3) + K_{T,\text{eff}} P_3, \tag{4.6}$$

$$\frac{\partial}{\partial t}F_3 = K_{F,\text{eff}} P_3, \tag{4.7}$$

$$\frac{\partial}{\partial t}E_3 = K_{E,\text{eff}} P_3, \tag{4.8}$$

where $D_{3,P,\text{eff}}$ is the effective diffusion constant, σ_S is the time scaling factor and $S = P, T$ and it can be defined as

$$\delta_S = \begin{cases} V_w + \frac{V_l}{K_P}, & x \in \text{water part of cytoplasm} \\ \frac{1}{K_P}, & x \in \text{membrane part of cytoplasm} \end{cases}$$

where V_w and V_l shows water and membrane parts of the cytoplasm respectively.

Sub-domain 5 (perinuclear space)

The perinuclear space consists of protein layers, P reacts with these proteins to form protein adducts thus giving rise to the following partial differential equations.

$$\frac{\partial}{\partial t}P_5 = \nabla \cdot (D_5 \nabla P_5) - (k_E + k_T)P_5, \tag{4.9}$$

$$\frac{\partial}{\partial t}E_5 = (k_E + k_T)P_5, \tag{4.10}$$

Sub-domain 7 (nucleus)

$$\frac{\partial}{\partial t}P_7 = \nabla \cdot (D_7 \nabla P_7) - (k_T + k_C + k_E)P_7, \tag{4.11}$$

$$\frac{\partial}{\partial t}T_7 = \nabla \cdot (D_7 \nabla T_7) + k_T P_7, \tag{4.12}$$

$$\frac{\partial}{\partial t}C_7 = k_C P_7, \tag{4.13}$$

$$\frac{\partial}{\partial t}E_7 = k_E P_7, \tag{4.14}$$

where C_7 and E_7 represent the DNA adducts and protein adducts respectively in the sub-domain 7. K_C and K_E stand for the reaction rate coefficients for the formation of DNA and protein adducts respectively.

TABLE 2. Chemical constants for the model

symbol	Constant	value
D_1	Diffusion constant in extra cellular medium	10^{-9}
D_2, D_4, D_6	Diffusion constant in membrane	10^{-12}
D_5, D_7	Diffusion rate in nucleus and peri-nuclear space	2.5×10^{-10}
$K_{p,P}$	Partition coefficient for P	1.2×10^{-3}
$K_{p,T}$	Partition coefficient for T	8.3×10^{-3}
$K_{F,Hom}$	GSH conjugate formation rate in homogenized cytoplasm	0.242908
$K_{T,Hom}$	Tetrol formation rate in homogenized cytoplasm	0.005744
K_E	Protein adduct formation rate	4.3×10^{-4}
K_C	DNA adduct formation rate	6.2×10^{-3}
K_T	Tetrol formation rate	7.7×10^{-3}
$K_{E,Hom}$	Protein adduct formation rate in homogenized cytoplasm	3.209×10^{-4}
$D_{P,eff}$	Diffusion rate in cytoplasm for P	4.06×10^{-10}
$\sigma_{P,Hom}$	Scaling factor for P	212.39
$\sigma_{T,Hom}$	Scaling factor for T	31.34
$D_{T,eff}$	Diffusion rate in cytoplasm for T	2.42×10^{-10}

Interface Conditions

The diffusion of species P and T takes place through membrane and water part. Due to the lipophilic nature of these species, these must be dissolved in membrane. Therefore, interface conditions are needed at the boundary. Moreover outward flux is equal to the inward flux because law of conservation of mass holds. To

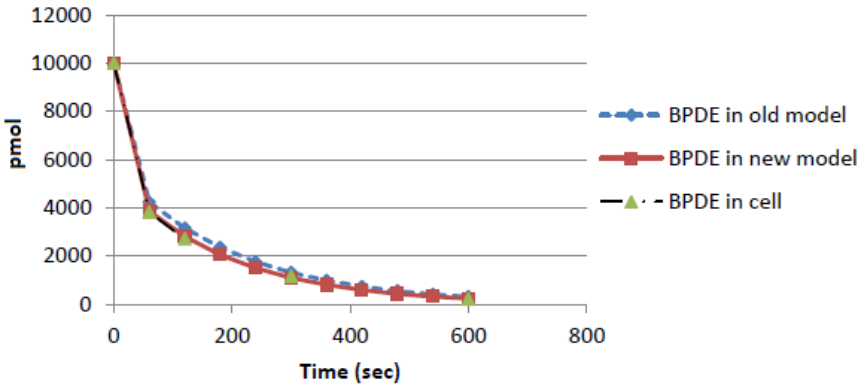

FIGURE 5.1. Degradation of Benzo(a)pyrene diol epoxide in extracellular region

describe the concentration at different boundaries between aqueous and lipid part the partition coefficient is introduced.

$$X_1 = K_{P,X} X_2 \qquad D_1 \frac{\partial}{\partial \mathbf{n}_1} X_1 = -D_2 \frac{\partial}{\partial \mathbf{n}_2} X_2$$

$$X_5 = K_{P,X} X_4 \qquad D_5 \frac{\partial}{\partial \mathbf{n}_5} X_5 = -D_4 \frac{\partial}{\partial \mathbf{n}_4} X_4$$

$$X_7 = K_{P,X} X_6 \qquad D_7 \frac{\partial}{\partial \mathbf{n}_7} X_7 = -D_6 \frac{\partial}{\partial \mathbf{n}_6} X_6$$

Boundary and Initial condition We suppose that the outer boundary of cell is isolated i.e there is no outward flux so Neumann boundary condition holds

$$\frac{\partial X_1}{\partial \mathbf{n}_1} = 0.$$

At the initial stage only P is present whereas all other species T, E, F, and C are set to zero. The concentration of P at initial stage is given by $P = P_0$.

5. Results And Discussion

The model is implemented in Comsol Multiphysics using reaction engineering lab [6-8]. This software works on the rules of finite element method [3]. UMFPACK method is used to solve the system of linear PDEs. UMFPACK method works on the principle of LU decomposition method [21].

The model was run for a time span of 600 sec, where the amount of molecules for different species in different subdomains was calculated. The comparison between the results of the previous and current extended model is shown in Figure (3.2-3.4).Fig. 3.2 represents the degradation of the concentration of BPDE. From the figure, it is shown that there was a minor difference in the results of old model and invitro data, whereas it shows very nice agreement when the comparison between the new model and the experimental data was made. The invitro data was obtained from [10].

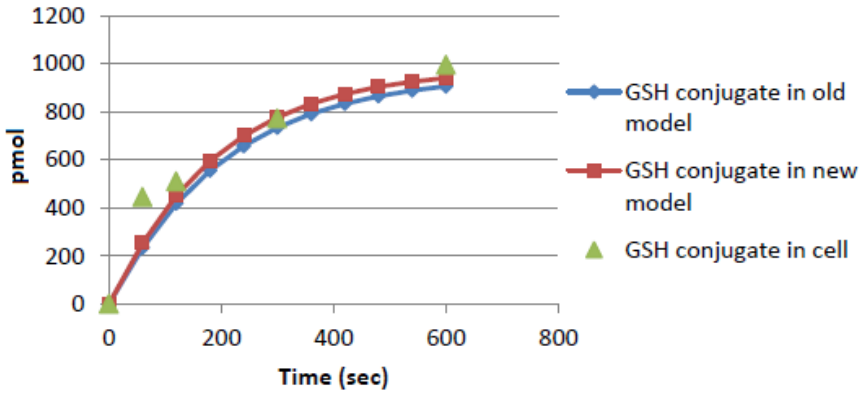

FIGURE 5.2. represents difference in the formation of GSH conjugates

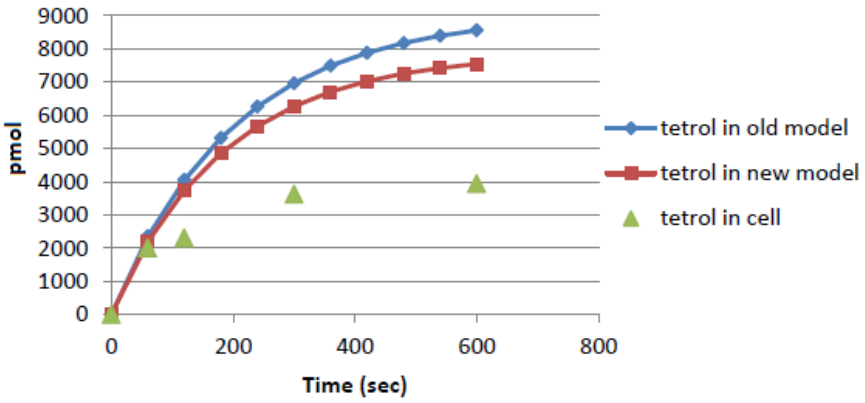

FIGURE 5.3. Formation of T (Tetrol)

As the volume of cytoplasm is increased BPDE will take more time to reach the nucleus. Hence more reaction will take place and it results a small difference in the formation of GSH conjugates. It shows that there is a slight increase in the concentration of GSH conjugate, which shows the betterment in the new model.

Fig. 3.4 shows the concentration of tetrol in cell. The difference found in the formation of tetrol inside the cell shows that the involvement of perinuclear space and protein reaction affects the formation of tetrol. The comparison of the results clearly shows that the results of the new model are much better than the results of the old model when compared with the experimental data. All the above clearly shows the significance of the new model. To find the optimal parameter for the model using optimization approach is an important work to be done as discussed by [4,12].

6. Acknowledgments

The authors acknowledge the support provided by University of Engineering and Technology, Lahore, Pakistan.

References

[1] N. Boffetta, *Cancer risk from occupational and environmental exposure to polycyclic aromatic hydrocarbons*, Cancer Causes Control **8**, (1997) 444-472.

[2] N. A. Campbell, B. Williamson and R. J. Heyden, *Biology: Exploring Life*, Pearson Prentice Hall, Boston, Massachusetts, 2006.

[3] J. Chaskalovic, *Finite element methods for engineering sciences*, Springer, Berlin Heidelberg, 2008.

[4] N. A. Chaudhry, M. O. Ahmad and J. Ali, *Constraint handling in genetic algorithms by a 2-parameter-exponential penalty function approach*, Pak. J. Sci. **61**, (2009) 122-129.

[5] P. Collas, *Nuclear Envelope Dynamics in Embryos and Somatic Cells*, Springer, US, 2002.

[6] COMSOL, *Chemical Engineering Module*, Stockholm, 2007.

[7] COMSOL, *Comsol Multyphysics 3.5a*, Stockholm, 2008.

[8] COMSOL, *Comsol Reaction Engineering Lab 1.5*, Stockholm, 2008.

[9] A. Cooper, A. Hewer, O. Ribeiro, P. Grover and P. Sims, *The enzyme-catalysed conversion of Anti-benzo[a]pyrene-7, 8-diol 9,10-oxide into a glutathione conjugate*, Carcinogenesis. **1**, (1980) 1075-80.

[10] K. Dreij, Q. A. Chaudhry, B. Jernstrom, R. Morgenstern and M. Hanke, *A method for efficient calculation of diffusion and reactions of lipophilic compounds in complex cell geometry*, PLoS ONE. **6**, (2011) DOI: 10.1371/journal. pone.0023128.

[11] K. Dreij, Q. A. Chaudhry, B. Jernstrom, R. Morgenstern and M. Hanke, *In silico modeling of Intracellular diffusion and reaction of benzo[a]pyrenediol epoxide*, KTH Royal Inst. of Technology **3**, (2012) 28.

[12] K. Dreij, Q. A. Chaudhry, J. Zhang, K. Sundberg, B. Jernstrom, M. Hanke and R. Morgenstern, *In silico modeling of the intracellular dynamics of polycyclic aromatic hydrocarbons*, ToxicolLett. **211**, (2012) S60-S61.

[13] R. G. Harvey, *Polycyclic Aromatic Hydrocarbons: Chemistry and Carcinogenicity*, Cambridge University Press, Cambridge, 1991.

[14] B. Jernstrom, J. Babson, P. Moldeus, A. Holmgren and D. Reed, *Glutathione conjugation and DNA binding of (+/2)-trans-7,8-dihydrobenzo[a]pyrene and (+/2)-7 beta,8alpha-dihydroxy-9 alpha,10 alpha-epoxy-7,8,9,10-tetrahydrobenzo[a]pyrene in isolated rat hepatocytes*, Carcinogenesis. **3**, (1982) 861-866.

[15] B. Jernstrom, M. Funk, H. Frank, B. Mannervik and A. Seidel, *Glutathione Stransferase A1-1-catalysed conjugation of bay and fjord region diol epoxides or polycyclic aromatic hydrocarbons with glutathione*, Carcinogenesis. **17**, (1982) 1491-1498.

[16] K. A. Ki-Hyun, A. J. Shamin, K. Ehsanul and J. C. Richard, *A review of air born polycyclic aromatic hydrocarbons (PAHs) and their human health effects*, Environment International **60**, (2013) 71-80.

[17] M. Moiz and J. George, *Toxicological Profile for Polycyclic Aromatic Hydrocarbons*, Revised ed. ATSDR, 1995.

[18] P. Paine, L. Moore and S. Horowitz, *Nuclear envelope permeability*, Nature. **254**, (1975) 109-114.

[19] K. Sundberg, K. Dreij, A. Seidel and B. Jernstrom, *Glutathione conjugation and DNA adduct formation of dibenzo[a,l]pyrene and benzo[a]pyrene diol epoxides in V79 cells stably expressing different human glutathione transferases*, Chem Res Toxicol. **15**, (2002) 170-179.

[20] D. R. Thakker, H. Yagi, W. Levin, A.W. Wood, A.H. Conney and D. M. Jerina, *Polycyclic aromatic hydrocarbons: Metabolic activation to ultimate carcinogens*, Academic Press, UK, 1985.

[21] A. D. Timothy, *UMFPACK Userguid ever*, 5.6.2, 2013.

[22] K. Townsend, A. Stretch, D. Stevens and D. Goodhead, *Thickness measurements on V79-4 cells: A comparison between laser scanning confocal microscopy and electron microscopy*, Int J Radiat Biol. **58**, (1990) 499-508.